
Proceedings Paper:
Gundogdu, B., Nejad, S., Gladwin, D.T. et al. (2017) A Battery Energy Management Strategy for UK Enhanced Frequency Response. In: Industrial Electronics (ISIE), 2017 IEEE 26th International Symposium on. 2017 IEEE 26th International Symposium on Industrial Electronics (ISIE), 19-21 Jun 2017, Edinburgh, UK. IEEE, pp. 26-31. ISSN: 2163-5137. EISSN: 2163-5145.

https://doi.org/10.1109/ISIE.2017.8001218

A Battery Energy Management Strategy for UK Enhanced Frequency Response

B. Gundogdu, S. Nejad, D. T. Gladwin, and D. A. Stone
Department of Electronic and Electrical Engineering
University of Sheffield
Sheffield, United Kingdom
bmantar1@sheffield.ac.uk

***Abstract*—Balancing the grid at 50 Hz requires managing many distributed generation sources against a varying load, which is becoming an increasingly challenging task due to the increased penetration of renewable energy sources such as wind and solar and loss of traditional generation which provide inertia to the system. In the UK, various frequency support services are available, which are developed to provide a real-time response to changes in the grid frequency. The National Grid (NG) – the main distribution network operator in the UK – have introduced a new and fast service called the Enhanced Frequency Response (EFR), which requires a response time of under one second. A battery energy storage system (BESS) is a suitable candidate for delivering such service. Therefore, in this paper a control algorithm is developed to provide a charge/discharge power output with respect to deviations in the grid frequency and the ramp-rate limits imposed by the NG, whilst managing the state-of-charge (SOC) of the BESS for an optimised utilisation of the available stored energy. Simulation results on a 2 MW/1 MWh lithium-titanate BESS are provided to verify the proposed algorithm based on the control of an experimentally validated battery model.**

Keywords— Battery Energy Storage; Enhanced Frequency Response; Grid Support; Lithium-Titanate

I. INTRODUCTION

Due to the high demand of electricity generation and the environmental concerns related to burning fossil fuels, there has been an increased uptake of renewable energy resources into the power transmission networks in the form of distributed generation (DG) [1]–[3]. However, intermittent renewables such as wind and solar introduce issues such as reliability, stability and power quality into the power grid. Energy storage systems (ESSs) are one of the efficient ways to tackle such issues by decoupling energy generation from demand [4]. Furthermore, ESSs can also be used to deal with the power quality concerns, especially in the UK, by providing ancillary services such as frequency regulation, 15-minute fast frequency response, operational reserve and load following [4], [5].

There are numerous types of existing ESS such as compressed air, fuel cells, hydrogen, cryogenic, pumped hydro, flywheel and superconducting magnetic storages [6]–[11]. In comparison to such ESSs, the battery energy storage system (BESS) has a number of benefits including storage size, energy efficiency, faster response time compared to conventional generation sources and low maintenance requirements [12], [13]. BESSs using different battery chemistries have been installed around the world for grid support (Table I).

TABLE I
LARGE-SCALE BESSS WITH GRID-SUPPORT APPLICATIONS

Type of BESS	Installation Sites	Facility Size Range	Potential/Actual applications
Lithium-Titanate	The University of Sheffield, (WESS), UK [12], [14]	2 MW, 1 MWh	– Frequency regulation – Peak shaving – Arbitrage
Lithium Iron Phosphate	Darlington, UK [14]	2.5 MW, 5 MWh	– Load shifting – Commercial ancillary services
Lithium-Nickel	Leighton Buzzard, UK [12], [14]	6 MW, 10 MWh	– Frequency support – Load shifting – Peak shaving
Valve-Regulated Lead acid	Lerwick Power Station, Shetland Island, UK [15]	1 MW, 3 MWh	– Demand peak reduction
Flooded Lead acid	Bewag, Germany [16]	17 MW, 14 MWh	– Frequency regulation – Spinning reserve
Nickel Cadmium (NiCd)	Golden Valley, Alaska [17]	40 MW, 4.7 MWh	– Electric supply reserve – Spinning reserve
Sodium-Sulphur (NaS)	Rokkasho, Japan [17]	34 MW, 220 MWh	– Renewables energy time-shift – Renewables capacity firming
Sodium Nickel Chloride (ZEBRA battery)	ZEBRA battery plant, Stabio, Switzerland [17]	40 MWh	– Mainly used in EV/HEVs
Vanadium- Redox Flow Batteries	GuoDian LongYuan Wind Power Co. China [18]	5 MW, 10 MWh	– Smoothing of wind power

In power distribution networks, the frequency is changing continuously due to the imbalance between demand and total generation; if generation surpasses demand, an increase in the grid frequency will occur and vice versa [19]. Balancing the grid at a nominal frequency (i.e. 50 Hz for the UK) requires managing many disparate generation sources against varying loads, which is becoming increasingly challenging due to the penetration of renewable energy sources and loss of traditional generation which provide inertia to the system. To overcome this issue, the National Grid (NG) – the main distribution network operator in the UK – is introducing a new faster frequency service, called Enhanced Frequency Response (EFR), that aims to maintain the system frequency closer to 50 Hz under normal operation [20]. For delivering such service to the grid, the BESS

is an ideal candidate. In the UK, there are limited numbers of installed BESS facilities that are suitable for providing grid frequency support. In 2013, the UK's first grid-tie lithium-titanate BESS, called the Willenhall Energy Storage System (WESS), was commissioned by the University of Sheffield to allow for research on large scale batteries and to create a platform for research into grid ancillary services.

In this paper, three different EFR service models are developed to evaluate control strategies for providing a real-time response to variations in the grid frequency. The first model introduces a new EFR service designed to meet the technical requirements of the NG Energy Transmission (NGET) specifications [20]. The second model covers the EFR service design with an extended 15-minute grid frequency event control, in order to optimise the utilisation of the available stored energy and to improve the EFR power delivery performance. Simulation results on a 2 MW/1 MWh BESS, namely the WESS plant in the UK, verify the transient performance of the proposed control strategy.

II. Enhanced Frequency Response Service

EFR is introduced as a new fast response service for grid balancing service that can provide 100% active power within 1second of registering a frequency deviation. NG prepared an EFR specification to facilitate a tender competition between potential energy storage providers in late 2016, which is explained in following sections.

A. Technical Requirements

Energy storage providers must respond to changes in nominal grid frequency (50 Hz) by increasing or decreasing their power output. Specifically, devices must deliver power to the grid to respond to changes in frequency outside of the dead-band (DB). Within the DB, there is not a requirement to deliver power to the grid [20] but there is opportunity within power limits to charge/discharge the battery to achieve a desired SOC.

B. Delivery Envelopes

Providers must deliver continuous power as described in one of the two EFR service envelopes in Fig. 1, Table II and Table III [24]. The providers must deliver their power within the upper and lower envelopes at all times; power delivered outside the envelope will lessen the service performance measurement (SPM) and hence availability payment [20]. In DB, the reference profile is at zero MW output and therefore providers do not need to respond to the system frequency. The BESS can be operated freely in DB but the maximum import/export power must not exceed 9% of the maximum power [20].

C. Ramp Rates

Providers may act within the lower and upper envelopes to deliver a continuous service to the system, with respect to the given limitations on ramp rates (see Fig. 2, Table IV and Table V) [20]. This is achieved by managing the battery's state-of-charge (SOC) in BESSs. For the zones A, C, D in Fig. 2, the ramp rate must obey the values in Table IV. Operation in C and D will cause penalties to the availability payment. Therefore, in such cases, EFR power output has to return to the envelope with respect to the given ramp-rate proportions (Table IV) [20].

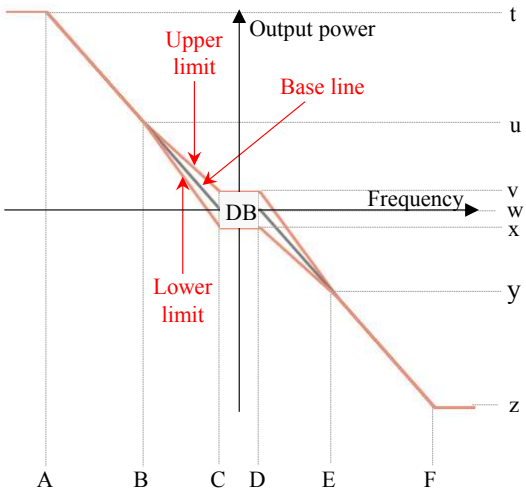

Fig. 1 EFR envelope [20]

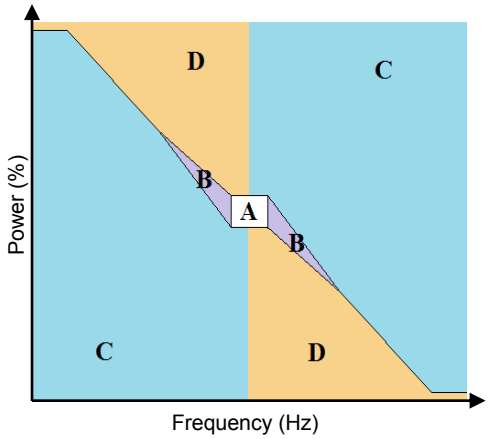

Fig. 2 EFR power zones [20]

TABLE II
EFR Envelope Frequency Boundaries [20]

Ref. Point	Service-1 (Hz)	Service-2 (Hz)
A	49.5	49.5
B	49.75	49.75
C	49.95	49.985
D	50.05	50.015
E	50.25	50.25
F	50.5	50.5

TABLE III
EFR Envelope Power Boundaries [20]

Ref. Point	Service-1 (%)	Service-2 (%)
t	100	100
u	44.44444	48.45361
v	9	9
w	0	0
x	-9	-9
y	-44.44444	-48.45361
z	-100	-100

TABLE IV
RAMP RATE AS A PRECENTAGE OF OPERATIONAL CAPACITY FOR POWER ZONES A, C AND D [20]

Area	Max Ramp Rate (MW/s)	Min Ramp Rate (MW/s)
A	1%	0%
C	200%	0%
D	10%	0%

Ramp-rate zone B is described as being the area between the lower and upper envelopes, excluding the DB, and extends to reach the full power capability at ±0.5 Hz [20]. The allowable ramp rates within zone B depend on the rate of frequency change. For Service-1 and Service-2, the ramp rate limitation for all frequencies in zone B is described in Table V. With these ramp limits, output power changes in proportion to changes in grid frequency, whilst allowing the energy storage providers some flexibility [20] to manage SOC.

TABLE V
RAMP RATE AS A PRECENTAGE OF OPERATIONAL CAPACITY FOR POWER ZONE B [20]

EFR Service	Max Ramp Rate (MW/s)	Min Ramp Rate (MW/s)
1 (wide)	$\left(-\frac{1}{0.45}\frac{df}{dt}+0.01\right)\times 100$	$\left(-\frac{1}{0.45}\frac{df}{dt}-0.01\right)\times 100$
2 (narrow)	$\left(-\frac{1}{0.485}\frac{df}{dt}+0.01\right)\times 100$	$\left(-\frac{1}{0.485}\frac{df}{dt}+0.01\right)\times 100$

III. EFR DESIGN CONTROL ALGORITHM

A. Model-1 Operational Principle

A new EFR control algorithm with a 2 MW/1 MWh BESS, called Model-1, is developed in MATLAB/Simulink to provide frequency response service to the NG (see Fig. 3). The BESS model used is verified against experimental operation of the WESS. Fig. 3 shows the EFR control scheme implemented in Model-1, where the inputs are frequency (f) and battery SOC, and the output is the required EFR power. The algorithm operates sequentially, where at each step in time, a set of power decisions are taken. The algorithm starts by detecting the position of the measured frequency with respect to the zones bounded by vertical lines 'A' to 'F' in Fig. 1. This is achieved by the 'EFR Power Calculation' block, where the required EFR response envelopes are calculated. In the 2 MW BESS model, the frequency and power bounds are calculated as a function of the limits denoted in Fig. 2, with their values declared in Table II and Table III. The power output is restricted to ±180 kW (9%) within the DB and both services include an upper, reference and lower power line denoted U, Z and L, respectively. The next block in the sequence selects the required power line with the decision being based on the measured SOC. For example, if the SOC is currently below a predefined limit, the demanded power is calculated using the equations derived for the lower line (L). This has the effect of either importing energy to charge the battery or minimising the exported energy to maintain a desired SOC range. The 'Zone Assignment' block is responsible for identifying the current operating zone (Fig. 2) for the calculation of the power-output levels. Finally, the change in power output per time step (1 second) for each zone is determined using the given ramp-rate limits in Table IV and Table V. In this work, battery SOC is calculated using,

$$\mathrm{SOC_{out}} = \mathrm{SOC_{init}} + \frac{\int_0^t P_{\mathrm{batt}} dt}{3600 \times Q} \qquad (1)$$

where $\mathrm{SOC_{init}}$, P_{batt} and Q represent initial SOC, instantaneous battery power and Watt-hour capacity, respectively.

B. Model-2 and Model-3 Operational Principle

The EFR specification defines frequency outside DB for longer than 15 minutes as an extended event whereby, after the 15 minutes it is optional to provide power for up to 30 minutes post the frequency returning to DB. In order to improve the BESS availability in Model-1, by reducing SOC limit events, an extended 15-minute grid frequency event control algorithm is implemented in EFR Model-2 and Model-3. Fig. 5 illustrates the logic of the two models.

Model-2 introduces a timed control block that measures the length of time that the frequency is continuously outside of the

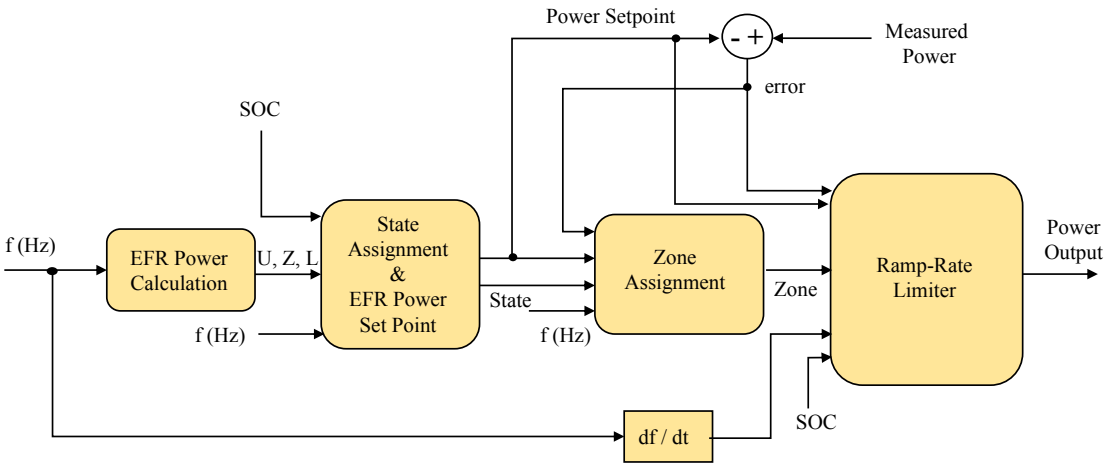

Fig. 3. Model-1 EFR control scheme.

DB. If this block measures a value greater than 15 minutes, then the output power of the BESS is set to zero. The BESS remains in this state until the frequency returns within DB, at which point a second timer starts timing for 30 minutes. Output power remains at zero until 30 minutes have elapsed, at which point the BESS resumes delivery of EFR according to the specification. Model-3 is extended to allow the BESS to manage its SOC during the 30-minute rest period by charging/discharging the battery within the ±9% power limit.

IV. EFR Models Simulation Results

The three EFR models are simulated in MATLAB/Simulink using real frequency data set obtained from NG. The simulation results provided in this paper are all based on a 1 MWh BESS model, which has been experimentally validated on the WESS plant in the UK, with a maximum EFR power of ±2 MW. The parameters used in the models are shown in Table VI.

A. Simulation Results of EFR Model-1

In order to demonstrate the performance of the reported EFR algorithm in Section III, the real frequency data for the 21st of October of 2015 is used herein, as this particular day is known to have a large period of under frequency. Fig. 4 shows the Model-1 simulation results for a 'Service-2' EFR. On the frequency plot, the DB is shown by the green lines.

TABLE VI
PARAMETERS USED IN EFR MODELS [20]

Parameter	Value
Nominal frequency	50 Hz
Low/high DB	±0.015 Hz (Service 2)
Max/min EFR power limit	±2 MW
Battery rated power/capacity	2 MW/1 MWh
Battery initial SOC (SOC_{init})	50%
SOC band (SOC_{low}- SOC_{up})	45-55%
Inverter efficiency (η_{inv})	97%
Battery coulombic efficiency (η_{DC})	94%

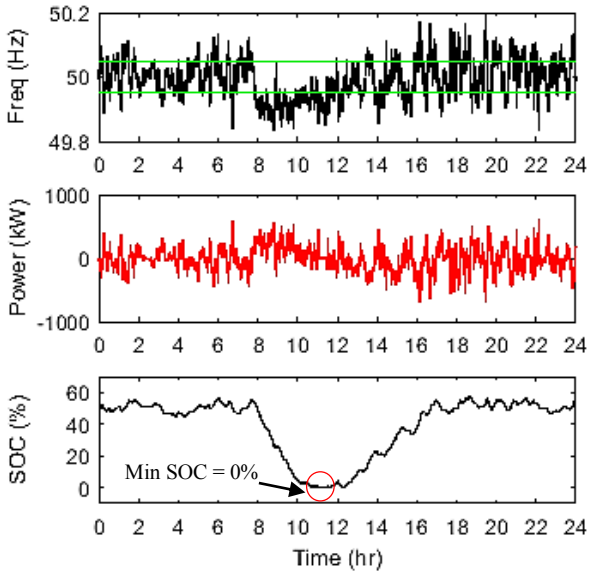

Fig. 4. Simulation results of EFR Model-1 for 21st Oct 2015.

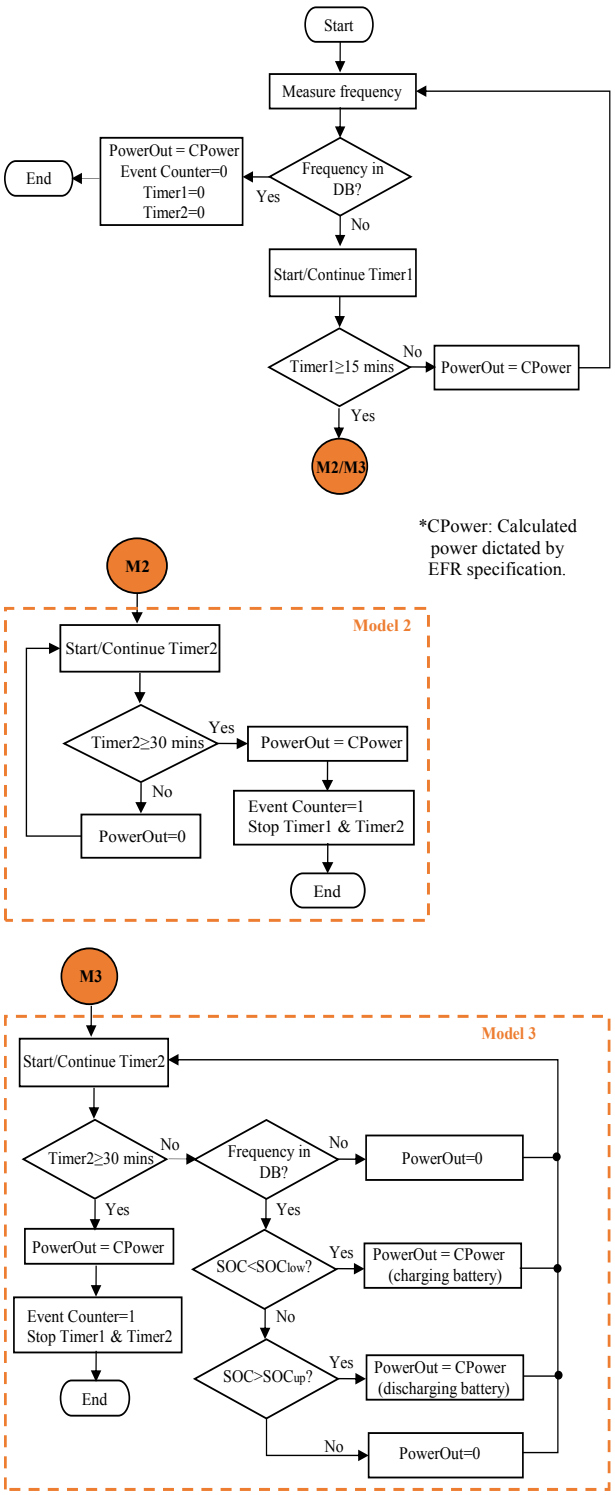

Fig. 5. Flow chart showing the structure of the two proposed batter energy management strategies for enhanced frequency response in the UK.

Over the period of 21st Oct 2015, the algorithm delivers to the EFR specification, whilst managing the SOC to the specified band of 45-55%. It can be seen that the SOC sharply decreases, reaching 0 % at 11.00 am, and remains there for ~30mins due to the frequency demands at that time. As the frequency stabilises, the algorithm charges the battery when it is allowed and restores the SOC to within the defined band.

Fig. 6 shows the power response versus frequency plot of Model-1 for 21st October 2015. The red lines represent the upper, lower and reference EFR power lines. It is clear that the power (blue circles) does remain within required zones of 'A' and 'B'. As outlined in Fig. 2, this is due to the SOC reaching 0% and hence there is no power available. This non-conformance would incur a penalty in payment and therefore it is necessary to improve the algorithm to minimise such occurrences.

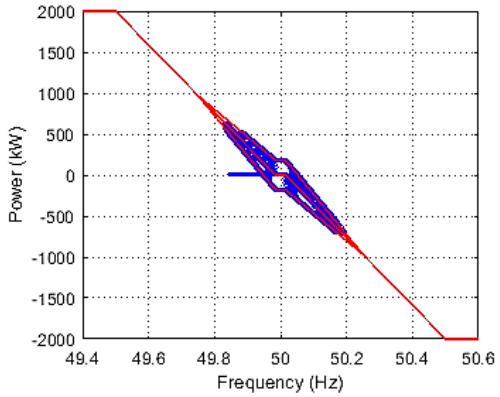

Fig. 6. EFR power response of Model-1 for 21st Oct 2015.

B. Simulation Results of EFR Model-2

Model-2 introduces the extended frequency event timer and cuts the power output after 15 minutes. The same frequency data is input to Model-2 capturing 13 15-minute extended frequency events. The results (Fig. 7) show that the lowest battery SOC reaches 30.7% compared to 0% in Model-1. The BESS is hence 100% available for delivering power according to the EFR specification (Fig. 8).

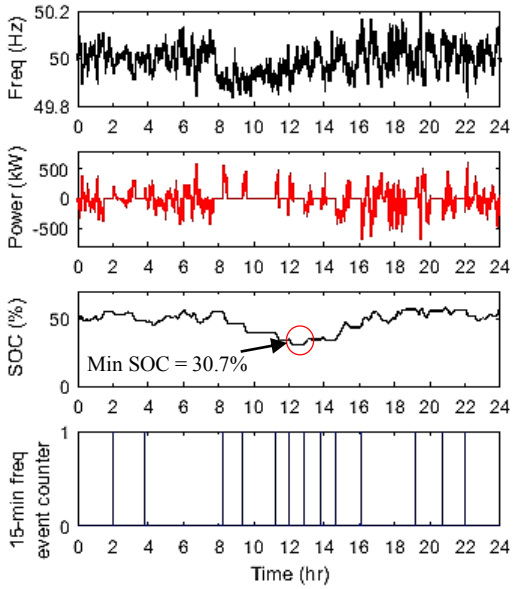

Fig. 7. Simulation results of Model-2 for 21st Oct 2015

C. Model-3 Simulation Results

The alogirthm in Model-3 allows for the charge/discharge of the battery during the 30-minute wait period. The model is simulated with the 21st October 2015 frequnecy data as shown in Fig. 9. The results demonstrate that again, the BESS provides 100% availability (Fig. 10) as seen with Model-2, however, the minimum SOC achieved with Model-3 is now 32.3%, compared to 30.7% of Model-2. This is a significant achievment in terms of optimised utilisation of the BESS available energy.

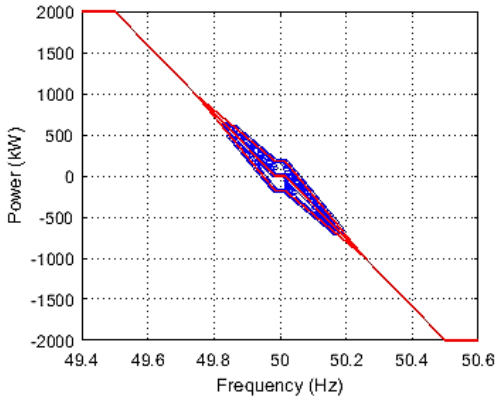

Fig. 8. EFR power response of Model-2 for 21st Oct 2015.

D. Analysis

In the EFR models it is possible to define two purposes for power flow in and out of the battery; the first is defined as that of charging/discharging the battery i.e. power is requested in either direction for the sole purpose of managing the SOC and not for EFR; the second is import/export which defines when the BESS is performing a mandatory response to a frequency event. The energy management findings of all EFR models are summarised in Table VII. It is clear that, by implementing the extended 15-minute frequency event control in Model-2 and Model-3, battery availability is increased from 98% to 100% (SPM); hence, this causes no availability penalties, which can offer substantial economic benefits to the battery providers.

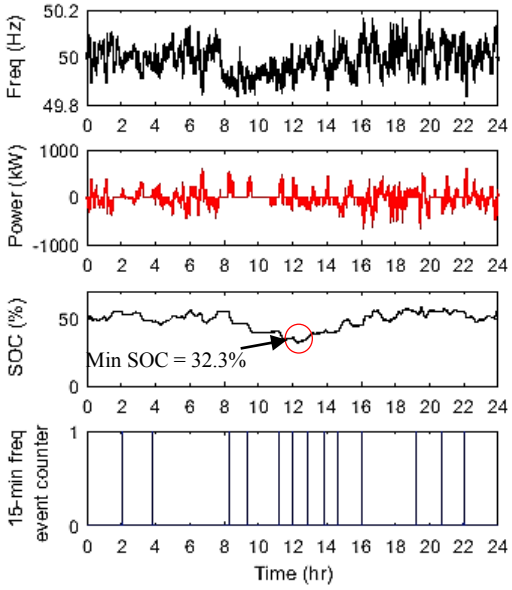

Fig. 9. Simulation results of Model-3 for 21st Oct 2015.

As desired, the battery SOC has been shown in the simulation results to converge on the selected band of 45-55% in all of the EFR models. In Model-3, the SOC converges faster

to the desired SOC band and it is predicted that this will minimise SOC excursions towards the limits, however, compared to Model-2 this is at the expense of using more energy, solely for SOC management (charge/discharge) within the DB. This is important as energy used outside of the DB (import/export) can be classified as Applicable Balancing Services Volume (ABSVD) and it is possible for this to be excluded by the provider i.e. zero cost. It should be noted that the reason for the different import/export energy in Model-2 and Model-3 is that, due to the difference in SOC, the BESS will not follow the same selection of EFR envelopes (Fig. 8 and Fig. 10).

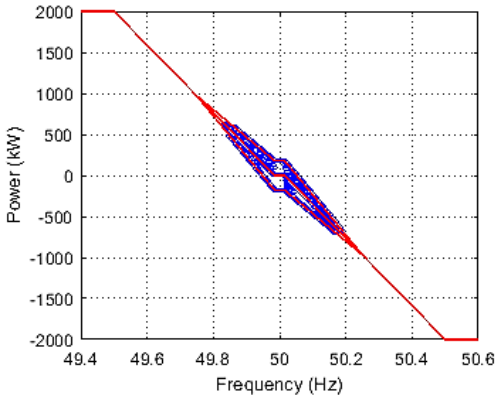

Fig. 10. EFR power response of Model-3 for 21st Oct 2015.

TABLE VII
ENERGY MANAGEMENT FINDINGS OF THE EFR MODELS

21st Oct 2015	Min SOC (%)	Max SOC (%)	SPM	Battery Charging Energy (kWh)	Battery Discharging Energy (kWh)	Battery Import Energy (kWh)	Battery Export Energy (kWh)	Total Energy (kWh)
M1	0	57.96	0.9828	160.6	83.33	1744	1470	3458
M2	30.67	57.8	1	63.48	71.2	1225	950.5	2310
M3	32.3	57.93	1	136.2	102	1185	957	2381

V. CONCLUSION

Three EFR algorithms based on a model of a 2 MW/ 1 MWh BESS have been developed to meet the NGET published requirements. When there is a deviation of frequency on the NG, the BESS provides a power response according to a specified EFR envelope. Simulations of the algorithms were carried out using NGET frequency data for 21st Oct 2015, which has the greatest number of continuous low frequency events. The simulation findings show that the EFR algorithms meet the UK's NGET EFR specification and successfully manage the SOC by converging towards a desired band of 45-55%. It was shown that for the basic algorithm that does not manage extended frequency events, the SOC sharply drops to 0% at 11.00 am and cannot continue to delivery an EFR service, resulting in a penalty. In order to improve the availability of the BESS, it is necessary to stop EFR after an extended 15-minute frequency event as allowed in the specification, with the results demonstrating 100% availability. Finally, the third algorithm demonstrated using the 30-minute wait period to manage the battery's SOC, resulting in a faster SOC convergence/recovery, however, there may be implications on the cost of energy supply as it would not be classed as being used for balancing services.

REFERENCES

[1] T. H. Mehr, M. A. S. Masoum, and N. Jabalameli, "Grid-connected Lithium-ion battery energy storage system for load leveling and peak shaving," in *Power Engineering Conference (AUPEC), 2013 Australasian Universities*, 2013, pp. 1–6.

[2] H. Qian, J. Zhang, and W. Yu, "A High-Efficiency Grid-Tie Battery Energy Storage System," vol. 26, no. 3, pp. 886–896, 2011.

[3] Y. Cho, J. W. Shim, S.-J. Kim, S. W. Min, and K. Hur, "Enhanced frequency regulation service using hybrid energy storage system against increasing power-load variability," in *Power and Energy Society General Meeting (PES), 2013 IEEE*, 2013, pp. 1–5.

[4] S. Vazquez, S. M. Lukic, E. Galvan, L. G. Franquelo, and J. M. Carrasco, "Energy Storage Systems for Transport and Grid Applications," *IEEE Trans. Ind. Electron.*, vol. 57, no. 12, pp. 3881–3895, Dec. 2010.

[5] X. Tan, Q. Li, and H. Wang, "Advances and trends of energy storage technology in Microgrid," *Int. J. Electr. Power Energy Syst.*, vol. 44, no. 1, pp. 179–191, 2013.

[6] K. C. Divya and J. Østergaard, "Battery energy storage technology for power systems—An overview," *Electr. Power Syst. Res.*, vol. 79, no. 4, pp. 511–520, Apr. 2009.

[7] S. Faias, P. Santos, J. Sousa, and R. Castro, "An overview on short and long-term response energy storage devices for power systems applications," *system*, vol. 5, p. 6, 2008.

[8] A. W. Bizuayehu, P. Medina, J. P. S. Catalao, E. M. G. Rodrigues, and J. Contreras, "Analysis of electrical energy storage technologies' state-of-the-art and applications on islanded grid systems," in *T&D Conference and Exposition, 2014 IEEE PES*, 2014, pp. 1–5.

[9] H. Chen, T. N. Cong, W. Yang, C. Tan, Y. Li, and Y. Ding, "Progress in electrical energy storage system: A critical review," *Prog. Nat. Sci.*, vol. 19, no. 3, pp. 291–312, 2009.

[10] H. L. Ferreira, R. Garde, G. Fulli, W. Kling, and J. P. Lopes, "Characterisation of electrical energy storage technologies," *Energy*, vol. 53, pp. 288–298, 2013.

[11] X. Luo, J. Wang, M. Dooner, and J. Clarke, "Overview of current development in electrical energy storage technologies and the application potential in power system operation," *Appl. Energy*, vol. 137, pp. 511–536, 2015.

[12] T. Feehally, A. J. Forsyth, R. Todd, M. P. Foster, D. Gladwin, D. A. Stone, and D. Strickland, "Battery energy storage systems for the electricity grid: UK research facilities," 2016.

[13] A. Joseph and M. Shahidehpour, "Battery storage systems in electric power systems," in *Power Engineering Society General Meeting, 2006. IEEE*, 2006, p. 8--pp.

[14] NGET, "Enhanced Frequency Control Capability (EFCC), Battery Storage Investigation Report," 2015.

[15] E. Gallant, "Lerwick Power Station Shetland Islands Case Study," 2017.

[16] W. C. Spindler, "Lead/acid batteries in utility energy storage and power control applications," *J. Power Sources*, vol. 35, no. 4, pp. 395–398, 1991.

[17] M. Świerczyński, R. Teodorescu, C. N. Rasmussen, P. Rodriguez, and H. Vikelgaard, "Overview of the energy storage systems for wind power integration enhancement," in *Industrial Electronics (ISIE), 2010 IEEE International Symposium on*, 2010, pp. 3749–3756.

[18] P. IRP, "Appendix L: Electrical Energy Storage," 2015.

[19] NGET, "Frequency Response Service," 2016. [Online]. Available: http://www2.nationalgrid.com/uk/services/balancing-services/frequency-response/.

[20] NGET, "Enhanced Frequency Response, Invitation to tender for pre-qualified parties V2.2," 2016. [Online]. Available: http://www2.nationalgrid.com/Enhanced-Frequency-Response.aspx.